Surface Charge of Bacteriorhodopsin Detected with Covalently Bound pH Indicators at Selected Extracellular and Cytoplasmic Sites†

Ulrike Alexiev,‡ Thomas Marti,§ Maarten P. Heyn,*,‡ H. Gobind Khorana,§ and Peter Scherrer‡

Biophysics Group, Department of Physics, Freie Universität Berlin, Arnimallee 14, D-14195 Berlin, Germany, and Department of Biology and Chemistry, Massachusetts Institute of Technology, Cambridge, Massachusetts 02139

Received August 20, 1993; Revised Manuscript Received October 25, 1993®

ABSTRACT: We present a method that allows the detection of the surface charge density of bacteriorhodopsin (bR) at any selected protein surface site. The optical pH indicator fluorescein was covalently bound to the sulfhydryl groups of single cysteine residues, which were introduced at selected positions in bR by site-directed mutagenesis. On the extracellular side, the positions were in the BC loop (72) and in the DE loop (129–134). On the cytoplasmic side, one position in each loop was labeled: 35 (AB), 101 (CD), 160 (EF), and 231 (carboxy tail). The apparent p*K*s of fluorescein in these positions were determined for various salt concentrations. The local surface charge density was calculated from the dependence of the apparent p*K* of the dye on the ionic strength using the Gouy–Chapman equation. The surface charge density at pH 6.6 is more negative on the cytoplasmic side (averaged over all positions, -2.5 ± 0.2 elementary charges per bR) than on the extracellular side (average, -1.8 ± 0.2 elementary charges per bR) with little variation along the surface. Since the experiments were performed with electrically neutral CHAPS/DMPC micelles, these values represent the charge present on bR itself. The validity of our approach is supported by the outcome of the following two control experiments: (1) when the positively charged surface residue Arg-134 was replaced by cysteine, the surface charge as detected by the indicator at that site became more negative by one elementary charge; (2) removal of the negatively charged carboxy tail on the cytoplasmic side reduced the negative charge density, as sensed by a pH indicator on the same side, but not on the opposite side. The contribution of the functionally important internal residues Arg-82 and Asp-96 to the surface charge density was determined using the double mutants G72C/R82A and V101C/D96A with the indicator dye attached to cysteine in position 72 and position 101, respectively. From the comparison of the charge density data obtained for the double mutants to the results for the single mutants G72C and V101C, it is concluded that Arg-82 contributes about 0.55–0.6 positive charge and Asp-96 0.6–0.65 negative charge to the surface charge on the membrane side to which they are closest.

Bacteriorhodopsin (bR),[1] the transmembrane protein of the purple membrane in *Halobacterium halobium*, contains a retinylidene chromophore attached to Lys-216 via a protonated Schiff base linkage and functions as a light-driven proton pump. Upon light excitation, bR undergoes a photocycle with several intermediates (J, K, L, M, N, and O) accompanied by the net transport of one proton from the cytoplasmic to the extracellular side of the purple membrane. In the first half of the photocycle, the Schiff base proton is transferred to Asp-85 (Braiman et al., 1988), and a proton is released to the extracellular medium. In the second half of the photocycle, the Schiff base is reprotonated from the cytoplasmic side, most likely via Asp-96 in the M to N transition (Gerwert et al., 1989; Otto et al., 1989; Tittor et al., 1989). The progress made toward an understanding of the mechanism of the light-driven proton pump bacteriorhodopsin has been reviewed (Mathies et al., 1991; Ebrey, 1993).

The surface charge density on either side of the purple membrane is of considerable importance for the proton translocation mechanism, as its value determines the local concentration of protons, the surface pH. The surface charge density of the purple membrane is negative (Jonas et al., 1990), and, consequently, the surface pH is lower than the bulk pH. The difference is salt-dependent and vanishes at very high ionic strength. The value of the surface charge, together with the salt concentration, thus determines the proton concentration at the surface. If the surface charge density differs on the two sides of the membrane, a pH gradient will exist even in the absence of proton pumping. If the surface charge density is nonuniform, the proton concentration will vary over the protein surface. A high local concentration of negatively charged surface groups on the cytoplasmic side of the membrane will lead, for instance, to a high local proton concentration on the surface, which may affect the proton uptake step. The surface proton concentration seems to play a major role in the kinetics of the photocycle and of proton uptake (Otto et al., 1989; Miller & Oesterhelt, 1990). Similar considerations hold for the proton release step.

In the past, various methods have been applied to measure the surface charge density of the purple membrane [for a review, see Jonas et al. (1990)]. The results are inconsistent

† This work was supported by a grant (Sfb 312-B1) from the Deutsche Forschungsgemeinschaft and a grant (03-HE3FUB) from the BMFT to M.P.H. and by a grant (AI 11479-18) from the National Institutes of Health to H.G.K.

* To whom correspondence should be addressed.

‡ Freie Universität Berlin.

§ Massachusetts Institute of Technology.

® Abstract published in *Advance ACS Abstracts,* December 15, 1993.

[1] Abbreviations: bR, bacteriorhodopsin; bO, bacterioopsin; DMPC, 1,2-dimyristoyl-*sn*-glycero-3-phosphatidylcholine; CHAPS, 3-[(3-cholamidopropyl)dimethylammonio]-1-propanesulfonate; MOPS, 4-morpholinepropanesulfonate; Tris, tris(hydroxymethyl)aminomethane; NG, nonyl β-D-glucopyranoside; DMPA, 1,2-dimyristoyl-*sn*-glycero-3-phosphatidic acid; EDTA, ethylenediaminetetraacetic acid; DTT, 1,4-dithio-DL-threitol; SDS, sodium dodecyl sulfate; IAF, 5-(iodoacetamido)fluorescein; C-AF, fluorescein bound to cysteine (cysteine-thio–acetamidofluorescein); pK_{app}, apparent p*K*; pK_t, true pK. The mutants are characterized by the replaced amino acids as follows: the letter before the number indicates the original amino acid in that position while the letter following the number represents the substituting amino acid using single-letter codes (e.g., V130C, valine in position 130 is replaced by cysteine).

0006-2960/94/0433-298$04.50/0

and vary from 0.5 to 9 negative elementary charges per bR. Moreover, it was not possible to distinguish between the two sides of the protein and obtain information on local variations.

In this paper, we present a method to determine the surface charge not only separately on either side of the protein but also at any desired position on the protein surface. The technique of site-directed mutagenesis made it possible to introduce a cysteine residue, which is absent in bR, into any desired position in the protein and to use the unique reactivity of the sulfhydryl group as a specific attachment site for various labels (Flitsch & Khorana, 1989; Altenbach et al., 1990). We have covalently attached the optical pH indicator 5-(iodoacetamido)fluorescein (IAF) to cysteine residues at selected positions on either surface of bR (Figure 1). Using the Gouy–Chapman equation, the surface charge density can be calculated from the dependence of the apparent pK (pK_{app}) of the dye on the salt concentration. With this straightforward approach, the following two questions were investigated: (1) Is the charge density uniform over the whole surface? (2) What is the value of the surface charge on either side of the membrane?

To test the validity of our method, presumably charged protein surface groups were removed or exchanged for neutral groups, and the effect on the surface charge density was determined. If the method is side-specific, the resulting changes in the surface charge should only be sensed by a label on the same side. When a negative charge is eliminated on the surface of the protein, a pH indicator on the same side should observe a more positive surface charge density, while an indicator on the opposite side should not be affected. The results expected for these control experiments were indeed observed, confirming the validity of the procedure. In a second set of experiments, internal residues, believed to participate in proton transport, were replaced (Arg-82, Asp-96), and changes in the surface charge density were detected with IAF attached to a cysteine residue on the extracellular side and the cytoplasmic side, respectively.

In our study, we used bR mutants expressed in *Escherichia coli* which were reconstituted in CHAPS/DMPC micelles. Under these conditions, one expects to measure the surface charge due to bR itself. With purple membrane, the negatively charged lipid headgroups will also contribute to the surface charge. Their contributions are difficult to estimate, since the glycosulfolipids are reported to be partially hydrolyzed (Kates et al., 1982) and the phosphatidylglycerophosphate headgroups are partially methyl-esterified (Tsujimoto et al., 1989). Moreover, complications may arise with purple membrane, since the surface charge increases during the titration due to the deprotonation of neighboring dye molecules. Both of these problems are absent with bR monomers containing only one dye molecule per micelle. The results of micelle experiments are thus expected to be easier to interpret. In summary, our approach presents a clear step forward and in principle allows the charge density to be mapped out over the entire surface of bacteriorhodopsin.

MATERIALS AND METHODS

Papain attached to agarose, 1,2-dimyristoyl-*sn*-glycero-3-phosphatidylcholine (DMPC), 3-[(3-cholamidopropyl)dimethylammonio]-1-propanesulfonate (CHAPS), 4-morpholinepropanesulfonate (MOPS), and tris(hydroxymethyl)-aminomethane (Tris) were obtained from Sigma. Nonyl β-D-glucopyranoside (NG) and 1,2-dimyristoyl-*sn*-glycero-3-phosphatidic acid (DMPA) were from Calbiochem. Ethylenediaminetetraacetic acid (EDTA), 1,4-dithio-DL-threitol (DTT), gluthatione (reduced), and sodium dodecyl sulfate (SDS) were from Fluka. Sephadex G-25 (fine) was from Pharmacia, and 5-(iodoacetamido)fluorescein (IAF) was from Molecular Probes.

Bacterioopsin Mutants. The construction of genes coding for the single and double mutants containing a unique cysteine residue, their expression in *Escherichia coli*, and the purification of the bacterioopsin apoprotein have been described (Altenbach et al., 1990; Marti et al., 1991).

Renaturation of bO. The isolated freeze-dried bO mutant protein (0.2 μmol) was dissolved in 1 mL of 1% CHAPS, 1% DMPC, 50 mM NaCl, 1 mM DTT, and 10 mM sodium phosphate buffer, pH 6.2, and regenerated by adding 0.25 μmol of *all-trans*-retinal and 4 M KCl to give 150 mM KCl. Excess lipids, detergents, and buffer were separated by chromatography on a Sephadex G-25 column preequilibrated and eluted with 0.1% CHAPS, 0.0025% DMPC, and 150 mM KCl.

IAF Labeling. 0.1 μmol of bR in 0.1% CHAPS, 0.0025% DMPC, 150 mM KCl, 4 μM EDTA, 0.1 mM DTT, and 50 mM Tris buffer, pH 8.0, was reacted with 1 μmol of 5-IAF for 30 min under argon. The reaction was stopped by addition of 20 μmol of glutathione; 2 μmol of DTT and the excess reagents were removed by chromatography on Sephadex G-25 in 0.1% CHAPS, 0.0025% DMPC, and 150 mM KCl. The labeling stoichiometry, molecules of fluorescein per molecule of bR, was determined spectroscopically using an extinction coefficient of $\epsilon = 68\,000\ M^{-1}\ cm^{-1}$ (Molecular Probes) for the alkaline form of fluorescein at 495 nm and of $\epsilon = 52\,000\ M^{-1}\ cm^{-1}$ for bR–micelles at 550 nm (London & Khorana, 1982).

Papain Cleavage. 0.05 μmol of bR in 0.1% CHAPS, 0.0025% DMPC, 150 mM KCl, 1 mM EDTA, 50 μM β-mercaptoethanol, 5 mM cysteine, and 20 mM MES buffer, pH 6.5, was reacted with 20 μL of activated papain (0.2 unit of papain attached to agarose suspended in 20 mM cysteine, pH 6.0, and 10 mM EDTA, pH 6.0, incubated for 30 min at room temperature) for 2 h at 40 °C. Papain was removed and the buffer medium changed by chromatography on Sephadex G-25 in 0.1% CHAPS, 0.0025% DMPC, and 150 mM KCl. The completeness of cleavage was verified by SDS–polyacrylamide gel electrophoresis (PAGE).

Titration Experiments. Prior to titrations, salt was removed from the bR–micelle solution by chromatography on Sephadex G-25 preequilibrated with 0.1% CHAPS, 0.0025% DMPC, and 10 mM KCl. The different salt concentrations were adjusted by adding 4 M KCl. The absorption spectra were measured with a Shimadzu 260 UV/VIS spectrophotometer equipped with an integrating sphere.

Analysis of Titration Data. The change in the absorbance, ΔA, of fluorescein at 495 nm was monitored as a function of pH. To obtain the apparent pK for fluorescein at each salt concentration, the data were fitted with the equation:

$$\Delta A = \Delta A_{max}/[1 + 10^{n(pK-pH)}] \quad (1)$$

ΔA_{max} is the maximal absorption difference between the acidic and the alkaline form of fluorescein, n is the number of protons involved in the transition, which should be 1 when only a simple protonation/deprotonation reaction takes place, and pK is the midpoint of the titration.

From the difference between the apparent pK (pK_{app}) at a given salt concentration and the intrinsic (true) pK (pK_t), the surface potential ψ was determined:

$$pK_t - pK_{app} = e\psi/2.3kT \quad (2)$$

The surface charge density σ was then calculated from ψ using

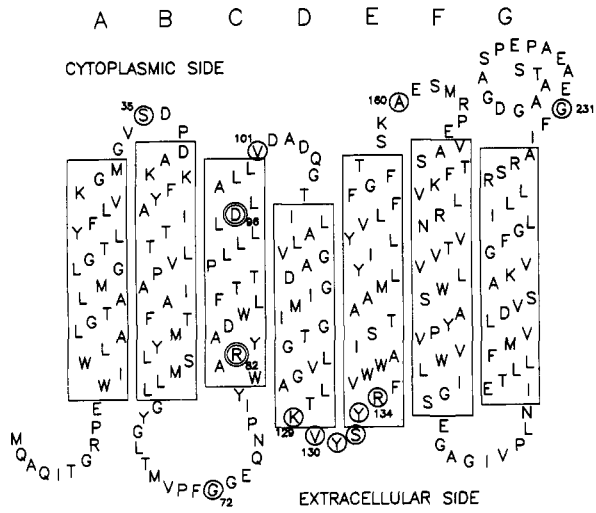

FIGURE 1: Secondary structural model of bacteriorhodopsin. The residues changed to cysteine are circled. The residues Arg-82 and Asp-96 which were also mutated are marked by a double circle.

the Gouy–Chapman equation:

$$\sinh e\psi/2kT = A\sigma C^{-1/2} \quad (3)$$

C is the salt concentration of the symmetric, monovalent electrolyte (KCl). A [$A = (8\epsilon\epsilon_0 N_A kT)^{1/2}$] equals 134.6 $M^{1/2}$ assuming a dielectric constant ϵ of 78.5 at 22 °C, ϵ_0 is the premittivity of free space, N_A is the Avogadro constant, and k is the Boltzmann constant. In the Gouy–Chapman plot, the surface potential is plotted versus the salt concentration according to eq 3, and the surface charge density is determined from the slope fitted by linear least-squares. Equation 2 requires the value of pK_t. At high electrolyte concentrations (≥2 M KCl), only a small residual surface potential remains. Thus, in principle, the pK_t may be determined using sufficiently high salt concentrations. However, the bR–micelles aggregate at salt concentrations above 1 M, preventing the determination of a reliable pK_t value in this way. Therefore, pK_t was calculated by extrapolation of the salt dependence of pK_{app} to infinite salt concentration with a transformed Gouy–Chapman equation (Koutalos et al., 1990). The pK_{app} value measured at 1 M KCl is approximately 0.2 pH unit higher than the calculated pK_t, a difference of the expected magnitude.

RESULTS

Labeling with (Iodoacetamido)fluorescein. Fluorescein was covalently bound to single cysteine residues in various positions on the extracellular and cytoplasmic surface of bacteriorhodopsin (Figure 1) using the iodoacetamide derivative (IAF). At pH 8, IAF reacted almost exclusively with the sulfhydryl group of cysteine. Within 30 min, about 0.7–1 mol of IAF was incorporated per mole of bacteriorhodopsin. In wild-type bR, without cysteine, less than 3% AF was attached under these conditions. The covalent binding of IAF was verified by the fluorescence of the bR band following SDS–polyacrylamide gel electrophoresis.

Spectral Characteristics of Fluorescein-Labeled bR. The absorption maxima of the bacteriorhodopsin mutants were identical to that of wild-type both before and after labeling. In addition, no differences, with respect to wild-type, were observed in the photocycle except for V101C, Y131C, and R134C, were only minor changes in the later part of the photocycle (M-decay) were detected. The size of the bR–micelle was estimated on the basis of time-resolved fluorescence

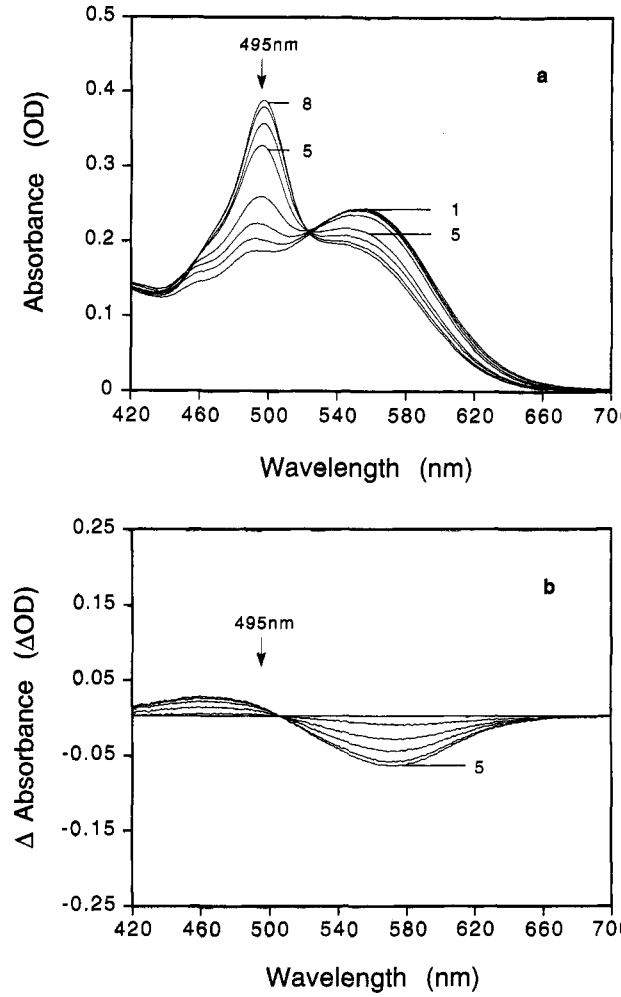

FIGURE 2: (a) Absorbance spectra of G72C-AF in 150 mM KCl at various pH values (curves 1–8: pH 5.5, 6.0, 6.5, 7.0, 7.5, 8.0, 8.5, and 9.0, respectively). The arrow in (a) and (b) is at 495 nm. (b) pH difference spectra of G72C in 150 mM KCl. The difference to the spectrum at pH 6.5 was plotted for pH (1) 7.0, (2) 7.5, (3) 8.0, (4) 8.5, and (5) 9.0.

anisotropy measurements (data not shown). The detected rotational correlation time of less than 50 ns corresponds to a spherical particle with a radius smaller than 3.8 nm. Since the bR–micelle most likely has an elongated shape rotating more slowly, a somewhat smaller size is expected than the one calculated. A particle of this dimension could contain only one or maybe two bacteriorhodopsin molecules.

Fluorescein has a pH-sensitive absorption spectrum with the maximum at 495 nm in the alkaline form. A typical set of absorption spectra at various pH values for bR with fluorescein bound to cysteine at position 72 on the extracellular surface is shown in Figure 2a. In addition to the dye absorbance changes, an alkaline transition also occurs for the bR absorption. For bR in CHAPS/DMPC micelles, the pK_{app} of the latter transition is lower than in purple membranes (Marti et al., 1991). As a control, the pH difference spectra of the mutant G72C not labeled with fluorescein are presented in Figure 2b. These difference spectra are characterized by a depletion maximum at 570 nm, a maximal absorbance increase at 465 nm, and an isosbestic point at 503 nm. Compared to the absorbance changes of fluorescein at 495 nm, the absorption differences due to the alkaline transition of bR at this wavelength are minimal. In the analysis of the dye absorbance changes, this contribution was neglected. The pH-dependent absorption spectra of all the other mutants

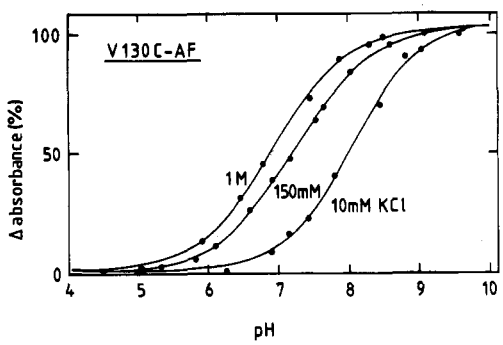

FIGURE 3: pH titration data of V130C-AF in 10, 150, and 1000 mM KCl and fitted curves. The absorbance changes at 495 nm in percent are plotted as a function of pH. For clarity, only the titrations at three different salt concentrations are shown.

Table 1: Surface Charge Densities per 1000 Å^2 and per bR Calculated from the Gouy–Chapman Equation for the Various Label Positions on the Surface[a]

label position on the surface	negative elementary charges per 1000 Å^2	negative elementary charges per bR	pK_t
extracellular			
G72C-AF	1.30–1.40	1.45–1.60	6.7
K129C-AF	1.65–1.75	1.90–2.00	6.9
V130C-AF	1.61–1.65	1.85–1.90	6.7
Y131C-AF	1.15–1.20	1.32–1.38	7.4
S132C-AF	1.50–1.55	1.70–1.80	6.7
Y133C-AF	1.45–1.50	1.67–1.72	7.4
R134C-AF	2.60–2.70	3.00–3.10	6.6
cytoplasmic			
S35C-AF	2.30–2.35	2.65-2.70	6.5
V101C-AF	2.30–2.35	2.65–2.70	6.4
A160C-AF	2.15–2.20	2.50–2.55	6.4
G231C-AF	2.10–2.20	2.40–2.55	6.4
double mutants			
G72C-AF/R82A	1.70–1.80	1.95–2.05	6.8
V101C-AF/D96A	1.75–1.80	2.00–2.10	6.6

[a] The true pK of fluorescein is given for each position.

used in this work (except for G72C/R82A and R82A) were quite similar to those shown in Figure 2 for G72C-AF.

When fluorescein was bound to the bR–micelle surface, its pK_{app} in 150 mM KCl was around 7.1–7.3, clearly higher than the pK_{app} of 6.3 determined for the unbound fluorescein. Moreover, the pK_{app} of the bound fluorescein was highly salt-dependent, whereas no salt dependence was detected for the unbound fluorescein. Figure 3 demonstrates as an example pH titration curves for V130C-AF at various salt concentrations. The pK_{app} decreased with increasing salt concentration by more than 1 pH unit, namely, from pK_{app} = 8.0 at 10 mM KCl to 6.9 at 1 M KCl. For all titration curves the number of protons involved in the transition was $n = 1 \pm 0.05$, indicating that in the pH range from 6.5 to 8 the protonation/deprotonation reaction of the dye is not affected by the deprotonation of other groups in the bR–micelle. The surface charge density appears to be constant in this pH range. The salt dependency of the apparent pK was used to calculate the surface charge density according to the equations described under Materials and Methods.

Surface Charge on the Extracellular and Cytoplasmic Side. The surface charge density was determined on the extracellular side with fluorescein bound to cysteine at positions 72 and 129–134 and on the cytoplasmic side at positions 35, 101, 160, and 231 (Figure 1). The results are summarized and presented as surface charge densities per 1000 Å^2 and per bR in Table 1. The surface area for the bR molecule was estimated to be 1150 Å^2 based on the projected density obtained

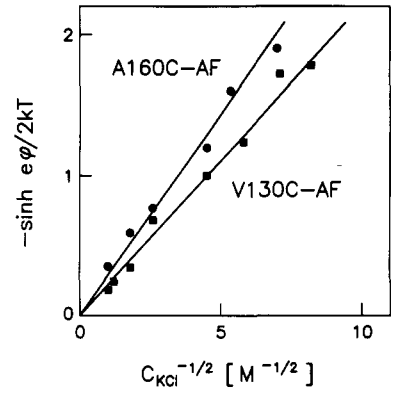

FIGURE 4: Gouy–Chapman plot of surface potential vs concentration of KCl according to eq 3 for (■) V130C-AF (extracellular side) and (●) A160C-AF (cytoplasmic side).

from electron diffraction data of the purple membrane (Henderson et al., 1990).

The charge densities on the extracellular side, determined in positions 130, 132, and 133 (1.7–1.9 e$^-$/bR), were quite similar. According to current models (Altenbach et al., 1990; Henderson et al., 1990) these residues are directly at the surface. In position 72, a smaller surface charge (1.5 e$^-$/bR) was detected. Gly-72 is located in the middle of the large BC loop and presumably removed from the surface (Figure 1). Therefore, a reduced surface potential effect on the label is to be expected in this position, and this may explain the smaller surface charge density calculated. Assuming that the difference in surface potential detected between position 130 (directly at the surface) and position 72 is entirely due to a distance effect, the distance between Gly-72 and the surface may be calculated from the linearized Poisson–Boltzmann equation. The result of approximately 4 Å appears quite reasonable. A smaller surface charge density was also determined for position 131. Residue 131 is located in the short DE loop (Altenbach et al., 1990), and, therefore, an explanation similar to that for position 72 does not hold. In addition to the reduced surface charge density, an unusually high pK_t value was obtained for this mutant. The pK_t values of the label in the various positions are shown in the last column of Table 1. For the positions on the extracellular side, the pK_t was approximately 6.7 except for Y131C-AF and Y133C-AF, where a value of 7.4 was obtained. The increased pK_t is probably due to a direct effect of a nearby negative charge. A possible explanation will be presented in the Discussion. The reduced surface charge density found in position 131 will be addressed in the same context.

For all positions on the cytoplasmic side (35, 101, 160, 231), a surface charge between 2.4 and 2.7 negative elementary charges per bR molecule was calculated (Table 1). The Gouy–Chapman plots for V130C-AF (extracellular) and A160C-AF (cytoplasmic) are presented in Figure 4, showing a clearly steeper slope for the cytoplasmic side due to its higher negative charge density. The fluorescein titration curves could be fitted with $n = 1 \pm 0.05$ for all mutants except for V101C-AF, where a value of approximately 0.8 was obtained. The titration data for V101C-AF in 75 mM KCl are shown in Figure 5. A break in the titration curve is apparent between pH 7 and pH 7.5. This break is reproducible and was observed in four different preparations of this labeled mutant. This suggests that some unknown group deprotonates in this pH range, thereby changing the surface charge density. Assuming that only one group deprotonates, one expects the observed broadened titration curve to be the superposition of two curves with $n = 1$. When the data were fitted accordingly, using the

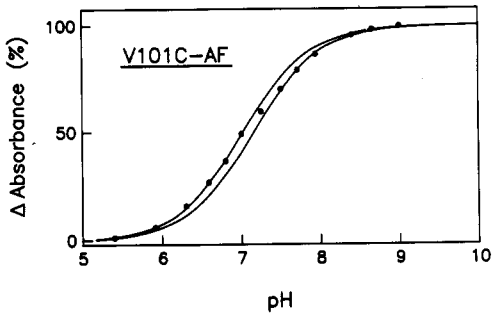

FIGURE 5: pH titration data of V101C-AF at 495 nm in 75 mM KCl. The absorbance changes at 495 nm in percent are plotted as a function of pH. The two fitted curves are obtained using the data points up to pH 7.0 and starting from pH 7.5 separately.

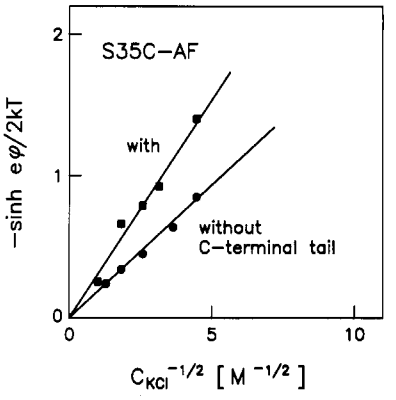

FIGURE 6: Gouy–Chapman plot for S35C-AF with (■) and without (●) the C-terminal tail.

points up to pH 7 for the first curve and the points starting from pH 7.5 for the second curve, an n value of ≈ 1 was obtained for the two curves (Figure 5). All titration curves for V101C-AF at the various salt concentrations show a similar break and were analyzed as explained, resulting in a higher and a lower pK_{app} value. The set of higher pK_{app} values leads to a surface charge of 2.65 e^-/bR, which is close to that in the other three positions on the cytoplasmic side (35, 160, 231). The lower pK_{app} values gave a reduced surface charge of approximately 1.7 e^-/bR. This difference of almost 1 charge indicates the deprotonation of a surface residue in this pH range. For each salt concentration, the break occurred approximately in the same position of the titration curve. We may thus conclude that the pK_{app} of the unknown deprotonating group has the same salt dependency as the pK_{app} of the dye and that this group senses the same surface charge as the dye. Since this break in the titration curve is only seen on the cytoplasmic side with AF in position 101, it is likely that the introduction of the AF molecule caused an increase of the pK_{app} of this particular surface group. The responsible groups could be the two aspartic acids Asp-102 and Asp-104. The required pK increase of an Asp to $\sim$7.5 may be caused by a closer proximity of these two aspartates to one another as a result of the fluorescein introduced in position 101.

The zwitterionic detergent CHAPS was exchanged for the neutral detergent nonyl glucoside (NG) in the mutant S35C to measure any possible effects by the detergent headgroup. The same surface charge density was obtained as for S35C-AF in CHAPS–micelles.

Removal of a Charged Amino Acid on the Surface. Very similar values for the surface charge densities were detected with fluorescein in the various positions on the same side of the membrane while a clear difference between the extracellular and cytoplasmic sides was observed. This suggests that a fairly homogeneous surface potential on either side of the protein was detected with the dye. If this is the case, then the replacement of a charged surface residue by a neutral amino acid should result in an equivalent surface charge change. On the extracellular side, Arg-134, expected to be positively charged at neutral pH, was replaced by Cys and fluorescein attached to this position. A surface charge of 3 e^-/bR was detected, about 1 unit more negative than the values of 1.7–1.9 e^-/bR obtained for the extracellular side (see Table 1; data not shown).

When Lys-129, which is also expected to be positively charged at neutral pH, was replaced by Cys, however, fluorescein in this position detected the same surface charge density of 1.9 e^-/bR as for other positions on the extracellular side. Thus, the exchange of Lys to Cys in position 129 did not result in a change of the surface charge density. This result may be due to an interaction of Lys-129 with Tyr-131 or Tyr-133 (see Discussion).

Contribution of the Charged C-Terminal Tail to the Surface Charge Density. As a further test, we removed the cytoplasmic tail containing five negative charges to examine the contribution of these charges to the surface potential. The tail was cleaved with papain in position 231 (Ovchinnikov et al., 1977) and separated by gel chromatography. Complete cleavage and removal of the C-terminal tail were verified by SDS gel electrophoresis. The effect of removing the charged tail on the surface charge density was determined with a label both on the cytoplasmic (S35C-AF) and on the extracellular (G72C-AF) surface. The labeled position on the extracellular side was used to test whether a charge change on one side of the protein is sensed on the opposite side. The surface charge density on the cytoplasmic side clearly decreased as is evident from the decrease in the slope in the Gouy–Chapman plot (Figure 6). The charge density was determined to be 1.5 negative charges per 1000 Å^2 or 1.7 negative charges per bR, a decrease of 0.8 e^-/bR. On the extracellular side (data not shown), no difference in the slopes of the Gouy–Chapman plots was observed, showing that the charge change is not sensed on that side.

Contribution of Ionizable Amino Acids Inside the Protein to the Surface Potential. The two internal residues Arg-82 (role in proton release) and Asp-96 (role in proton uptake) were replaced by Ala. The surface potential was detected with fluorescein bound to Cys in position 72 for R82A and in position 101 for D96A. These two double mutants, G72C/R82A and V101C/D96A, have photocycles similar to those of the single mutants R82A and D96A (Alexiev et al., unpublished results). The labeling of Cys with fluorescein had in both cases no further effect on the photocycle. The removal of Arg-82 inside the protein increased the negative surface charge density detected in position 72 from 1.45–1.6 to 1.95–2.05 e^-/bR (Table 1). The difference in the slopes of the Gouy–Chapman plots for G72C-AF and G72C-AF/R82A (Figure 7) is apparent. Replacing Arg-82 by Ala caused a charge difference at the extracellular protein side of about 0.6 e^-/bR. This result is similar to that obtained for the removal of the positively charged residue Arg-134, indicating that Arg-82 is also positively charged. The absorption maxima of the single and double mutants R82A and G72C/R82A are red-shifted to 585 nm in 150 mM KCl at pH 6.0. This blue state is similar to the blue form of wild-type with the pK_{app} of the transition shifted from approximately 4.7 to 7.2 for micelles in 150 mM KCl. The pK_{app} of this blue to purple transition is ionic strength dependent. When the pK_{app} data for this transition of G72C/R82A were also analyzed

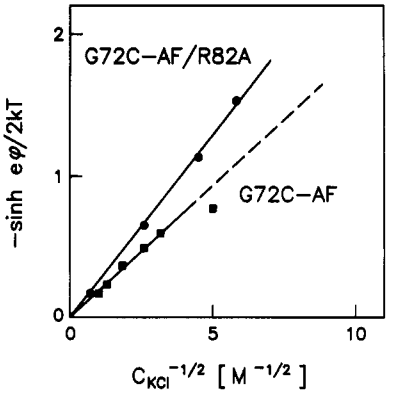

FIGURE 7: Gouy–Chapman plot for (■) G72C-AF and (●) G72C-AF/R82A.

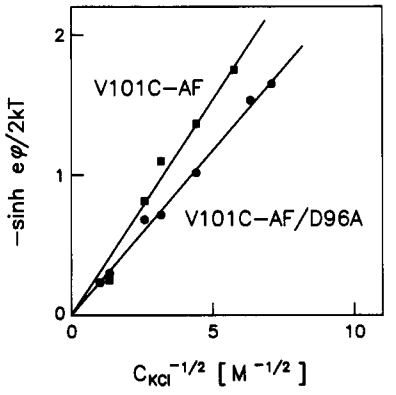

FIGURE 8: Gouy–Chapman plot for (■) V101C-AF and (●) V101C-AF/D96A.

according to eq 2 and 3, a Gouy–Chapman plot with a straight line going through the origin was obtained (data not shown), and a charge density of 2.3–2.45 e^-/bR was calculated. The true pK for the blue to purple transition was at 6.5. The calculated charge density from this transition agrees with the one obtained for the extracellular surface in this mutant.

The slope of the Gouy–Chapman plot for the mutant D96A/V101C-AF with the label on the cytoplasmic side (Figure 8) yields a surface charge density of 2.10 e^-/bR. This represents a charge decrease of about 0.6 elementary charge compared to the value estimated for V101C-AF. The same break in the titration curves as for the single cysteine mutant V101C-AF was detected. Therefore, the same method was used for both analyses. The same charge difference was obtained when either the titration data points below or above the break or all points together were analyzed.

DISCUSSION

The values previously reported for the surface charge density vary from 0.5 to 9 negative charges per bR molecule [0.5 e^- (Packer et al., 1984); 2 e^- (Ehrenberg et al., 1989); 9 e^- (Renthal & Cha, 1984)]. The methods used to determine the charge density did not allow one to distinguish between the two protein surfaces, their reliability could not be tested, and the contribution of charged phospholipid headgroups to the detected surface potential was difficult to estimate.

To determine the surface charge density, the apparent pK of the pH indicator fluorescein, covalently attached to selected positions on the extracellular and cytoplasmic protein surface, was measured in CHAPS/DMPC micelles as a function of the salt concentration. The mutation to a cysteine residue and the introduction of the label did not cause a change in the absorption maximum of bR and had no or only minor effects on the later part of the photocycle (unpublished observations). Our approach to measure the surface charge of bR in CHAPS/DMPC micelles has the following advantages: (1) the exact position of the pH-sensitive dye is known; (2) the indicator can be moved to any desired protein surface position; (3) interactions between dye molecules are absent (charges of neighboring dye molecules), as indicated by the n values of 1 obtained for the titration curves; and (4) only the charges from amino acid side chains of bR are measured in the absence of contributions from the charged phospholipid headgroups of the purple membrane. Since bR monomers incorporated into lipids with overall neutral headgroups are functional (Szundi & Stoeckenius, 1988), the charged lipid headgroups present in purple membranes cannot be a prerequisite for function. The conformation of bR in micelles might not be identical to the one in purple membrane, but its function is retained as seen by the light-induced proton release and uptake similar to purple membrane (data not shown). The zwitterionic detergent CHAPS had no effect on the surface potential as seen following its replacement with the uncharged detergent nonyl glucoside.

The observed increase in the pK_{app} for the alkaline transition of fluorescein bound to the bR surface compared to the unbound molecule can be the result of either a direct charge interaction between fluorescein and a negatively charged group in its immediate vicinity and/or a negative surface potential of bR caused by an overall net negative charge of the surface residues. The latter results in an ionic strength dependent surface potential and determines the proton concentration at the surface. Only at high salt concentrations does the surface pH equal the bulk pH, at which point the apparent pK of the bound dye should be equal to the pK of the unbound molecule. The decrease in the observed pK_{app} of the bound fluorescein with increasing ionic strength in the medium to a value close to that of the unbound dye at very high salt concentrations suggests a surface potential effect.

The dependence of the surface potential on the surface charge and on the bulk ionic strength is described for the case of a 1:1 electrolyte by the Gouy–Chapman equation (eq 3). This one-dimensional theory assumes that the charge density is uniformly distributed on an infinite plane. Strictly speaking, the assumptions on which the Gouy–Chapman equation is based are not valid for our system of bR monomers incorporated in micelles. Nevertheless, in most cases, where the Gouy–Chapman approximation was used for biological membranes or vesicles with discrete charges from amino acid side chains and membrane lipids, surprisingly good results were obtained [for a review, see Cevc (1990)]. This is indicated, among other things, by internal consistencies in the data analysis, e.g., Gouy–Chapman plots with straight lines going through the origin. The analysis of our experimental data shows good linearity in the plots for salt concentrations between approximately 1 M and 30 mM. Moreover, the straight lines obtained go through the origin as required by eq 3. A deviation from linearity is observed only for salt concentrations lower than 30 mM KCl. This may be due in part to the unavoidable fact that during the pH titration the salt concentration is altered when aliquots of KOH are added. In one titration, about 3 mM salt was added. This effect becomes significant at salt concentrations below 20 mM and leads to nonlinearities in the Gouy–Chapman plots in this region.

The finite size of the surface area of bR could be another cause for the nonlinearity at low salt concentrations. Data analysis on the basis of the Gouy–Chapman theory will become problematic when the Debye length is equal to or larger than

the diameter of the bR surface area. The Debye length at 10 mM KCl equals 30.4 Å and is thus approximately the same as the bR diameter of about 35 Å. Since the Debye length decreases with 1 over the square root of the salt concentration, it becomes much smaller than the bR diameter at higher salt concentrations. Another questionable point in the data analysis concerns the value of 78.5 used for the dielectric constant. In the interface region between the aqueous bulk and the hydrophobic protein interior, the dielectric constant varies from 78.5 to perhaps ≈10 (Cevc, 1990). Since the surface charge density is inversely proportional to the square root of the dielectric constant, a smaller dielectric constant leads to a higher calculated surface charge density. For example, when the dielectric constant is decreased from 78.5 to 60, a surface charge density of 1.70 e^-/bR increases to 1.96 e^-/bR. Because of its size and somewhat polar character, we expect that fluorescein resides in an aqueous region and assume a dielectric constant of 78.5.

The effect of salt on the pK_{app} of fluorescein, bound to various positions on the same protein surface, is about equal. Therefore, the corresponding surface charge densities are also approximately the same. However, there is clearly a charge difference between the two surfaces. The uniform potential sensed by the indicator molecule on each side is not too surprising because of the size and rotational freedom of the fluorescein. The dye molecules, which are attached to cysteines in the loop regions, are expected to have considerable rotational flexibility around axes both parallel and perpendicular to the surface. Evidence for this comes from time-resolved fluorescence depolarization experiments (data not shown). The surface potential felt by the dye thus represents the average over the area sampled during this motion. This lateral averaging would tend to reduce local variations in the surface charge density. Since the titratable OH group of the dye is located opposite the reactive iodoacetamide group, the potential is probably determined a few angstroms away from the surface. If this assumption is correct, the actual surface charge would be somewhat more negative than calculated. On the basis of similar considerations, the smaller surface potential detected by the dye in the extracellular position 72, compared to the other extracellular positions 130 and 132, was interpreted as an increased distance of the dye from the protein surface by approximately 4 Å. The surface charge density for the extracellular side was calculated to be 1.8 ± 0.2 e^-/bR, clearly less negative than the value obtained for the cytoplasmic side (2.5 ± 0.2 e^-/bR).

As noted under Results, the area of bR was estimated from the projected area in electron density maps of purple membranes. This area represents the average over all in-plane cross sections of the protein. The error of this estimate is about 12%. The area in micelles is expected to be equal or slightly larger for a possibly somewhat looser structure. We assumed the same area for both surfaces. With these assumptions, the charge difference between the two sides of the protein is only 0.5–1 e^-/bR. This is in agreement with measurements of the permanent dipole moment of bR in purple membranes, which suggest only small differences in the surface charge density between the two sides of the membrane (Kimura et al., 1984; Taneva et al., 1987).

The pK of 6.3 determined for fluorescein in solution is somewhat lower than the true pK values calculated for the bound fluorescein on either side of the protein. Furthermore, there is a small (0.3 unit) difference between the pK_t values on the extracllular versus the cytoplasmic side. The cause for this difference is unknown. Except for Y131C-AF and Y133C-AF (to be discussed below), the true pK values found in the various positions for each side are about equal. This suggests that if salt-independent charge interactions with the dye exist, their effect does not vary with position.

The removal of charged groups on either protein surface (Arg-134, C-terminal tail) is sensed by the dye as a change in the surface potential equivalent to a charge change of approximately one positive charge for Arg-134 and slightly less than one negative charge for the C-terminal tail. The overall contribution to the surface potential of the cleaved tail is about two negative charges, since the carboxyl group of the C-terminal residue in the cleaved protein must be accounted for. The relatively small contribution of the C-terminal tail indicates that this region, with its five negative charges, is not structured on the surface in bR micelles but more or less free in the aqueous phase. Moreover, these charges do not seem to be essential for the function of bR, since cleaving the C-terminal tail affects neither the photocycle kinetics nor the proton pumping activity (data not shown). The removal of the C-terminus does not alter the surface potential on the opposite side as shown with a label bound to the extracellular side. Therefore, we can exclude a contribution of charged residues from one protein surface to the other. The surface charge densities determined are side-specific. The changes in the surface charge densities, calculated from the detected surface potential changes following the charge changes introduced on the surface, agree with the charges actually removed. This supports our conclusion that the ionic strength dependent pK_{app} effects of the dye are indeed caused by the surface potential and that the analysis applying the Gouy–Chapman equation is valid.

One apparent disagreement, however, remains. In contrast to the results for Arg-134 and the negatively charged C-terminal tail, the exchange of Lys-129 (expected to be positively charged) to Ala does not lead to a detectable surface charge change. One possibility is that Lys-129 is not charged. Alternatively, its charge may be neutralized by a negative charge from another amino acid side chain, and once Lys-129 has been removed, this group becomes protonated, resulting in no detectable charge change. The first possibility is unlikely since Lys-129 is expected to be near the surface (Altenbach et al., 1990). For the latter explanation, one could consider as possible group(s) to interact with Lys-129 one or both of the two tyrosines in positions 131 and 133. The proximity of the positively charged lysine to a tyrosine could result in a decreased pK_{app} for the hydroxyl group providing a negative charge. Since no other titratable group besides the dye was detected, the pK_{app} of the tyrosine should be near 6.5, below the titration range used to determine the pK_{app} of the dye. Such an interaction between Lys-129 and the Tyr-131 or/and Tyr-133 could explain several of our observations at the same time (no charge change upon removal of Lys-129, reduction of the negative surface charge density upon changing Tyr-131 or Tyr-133 to Cys, elevated pK_t values for the dye in positions 131 and 133) as follows: (a) removal of Lys-129 results in a normal pK_{app} for Tyr-131 and/or Tyr-133, and therefore no net charge change is detected; (b) by replacing either Tyr-131 or Tyr-133 with a Cys carrying the dye molecule, the positive charge on Lys-129 can no longer be fully neutralized and a decreased negative surface charge density is observed mainly in position 131; (c) the proximity of the remaining tyrosine with its partial negative charge to the dye molecule increases the true pK of the dye.

The changes in charge density observed with the indicator on the surface following the removal of internal charges are

more difficult to interpret than those for surface charges. The contribution of a charged amino acid side chain inside the protein to the surface potential will depend on the distance between the residue and the membrane surface and on the dielectric constant for the region between the charge and the surface. The dielectric constant in membrane proteins can be as low as 4–10 and is not expected to be homogeneous. Structural investigations suggest the existence of a proton channel containing a number of water molecules (Henderson et al., 1990; Papadopoulos et al., 1990). An environment with a high dielectric constant would negate a portion of the internal charge at the surface. Therefore, the difference in the surface charge density obtained after removal of an ionized amino acid inside the protein may represent only a fraction of the actual changed charge. A charge change in the interior of the protein could have a destabilizing effect (lack of ion pair, changes in hydrogen bonding), causing a structural change that could result in an altered contribution of other charged amino acids to the surface potential.

Fluorescein, in position 72, senses an increased negative surface charge density when Arg-82 is replaced by Ala, and this increase is equivalent to a charge change of 0.4–0.5 e^-/bR. As discussed above, Cys-72 is not located directly at the surface, and the charge change normalized to the surface is 0.5–0.6 e^-/bR. Assuming that through the mutation only the positive charge of Arg-82 was removed and no other charge changes (due to conformational changes) occurred, we conclude that Arg-82 is positively charged in the ground state at neutral pH. Provided Arg-82 is a member of an ion pair, the detected potential change would have as its source the remaining negative charge. There is considerable evidence for a charge interaction of Arg-82 with the negatively charged residue Asp-85 (Stern & Khorana, 1989; Otto et al., 1990). It has also been suggested that Arg-82 together with Asp-85 and Asp-212 forms a complex counterion to stabilize the protonated Schiff base, a neutral quadrupole (de Groot et al., 1990; Der et al., 1991; Marti et al., 1991; Ormos et al., 1992). In either case, the potential increase would be from the remaining complex ion or from one of the aspartates. It is believed that even ion pairs inside the hydrophobic domain of a protein need to be further stabilized by interactions with polar groups or/and hydrogen bonds (Honig & Hubbell, 1984; Warshel et al., 1984). If such a hydrogen-bonding network exists, then even an internal charge can be effectively delocalized. An indication for this type of interaction is actually the purple-to-blue transition where the proton concentration at the surface seems to directly affect the charge distribution near the Schiff base, causing the color change (see below).

The pK_t for the purple-to-blue transition of 6.5 detected in the mutant protein R82A and R82A/G72C in micelles is 2.2 pH units higher compared to wild-type in micelles (our unpublished observation) and similar to the one determined for R82A incorporated into lipid vesicles in 2 M KCl (pK_{app} = 6.4; Subramaniam et al., 1990). The surface charge density calculated from the ionic strength dependence of the purple-to-blue transition in R82A/G72C and R82A/G72C-AF of about 2.4 e^-/bR is equal to the surface charge density determined on the extracellular side with fluorescein in R82A/G72C-AF. It is unlikely that this coincidence is accidental and it suggests a direct relationship between the purple-to-blue transition and the surface potential on the extracellular side. The increased negative surface charge density of 0.6 unit in the mutant R82A/G72C is too small to account for the increase in the pK of the purple-to-blue transition of more than 2 units. The red-shift in the chromophore absorbance could be caused either by a structural change modifying the geometry of charges near the Schiff base or by protonation of a group in its vicinity. A decrease in the surface pH could be the reason in both cases (Szundi & Stoeckenius, 1989). Since the titration curves for the purple-to-blue transition at the various salt concentrations could be fitted with an n value of about 1, indicative of a one-proton reaction, protonation of a single residue seems to be quite likely. Because an n value of approximately 1 was also obtained for the titration curves of fluorescein in R82A/G72C-AF, there is no detectable change in the surface charge density on the extracellular side in the purple-to-blue transition between pH 6.5 and 8.0. Thus, the charge of a residue protonating in the purple-to-blue transition does not contribute to the surface potential, implying an internal location possibly near the Schiff base. There is considerable evidence that Asp-85 is the residue protonating in this transition: all the mutants with Asp-85 replaced by a neutral amino acid are red-shifted at neutral pH (Mogi et al., 1988), and the ^{13}C-NMR spectra of the blue form of bR suggest that Asp-85 is protonated (Metz et al., 1992). Arg-82 may have a stabilizing role in the structure, and/or its charge could have an effect on the pK of the protonating group Asp-85 in the purple-to-blue transition.

The double mutant V101C/D96A shows the same characteristics in the photocycle as the single mutant D96A, and both have an absorbance spectrum similar to the wild-type protein. Amino acids with normally charged side chains at neutral pH can be incorporated into hydrophobic domains as ion pairs or as ions that are stabilized by a network of hydrogen bonds and polar amino acids. Data obtained by FTIR spectroscopy are interpreted to indicate that Asp-96 is protonated in the bR ground state (Braiman et al., 1988). On the basis of structural studies, Asp-96 is believed to be located in a relatively hydrophobic environment, approximately 7 Å from the cytoplasmic surface and 10 Å from the Schiff base (Henderson et al., 1990). If nonionized Asp-96 is replaced by a neutral amino acid, one would not expect to detect any potential change on the surface. However, when Asp-96 is replaced by Ala, we detect in position 101 on the cytoplasmic side a decreased negative surface charge density which is equivalent to a charge change of 0.6 e^-/bR. The actual charge difference may be larger because of the distance effect and dielectric constant discussed earlier. This decreased negative charge density detected on the cytoplasmic side in D96A/V101C-AF compared to V101C-AF indicates Asp-96 to be negatively charged in the bR ground state. The titration curves have all an n value of 1, showing the absence of a charge change in the titration range of pH 6.5–8.5. Therefore, the pK_{app} for Asp-96 must be lower than pH 6.5. We cannot rule out entirely the possibility that a protein structural change modified the contribution from other charged groups to the surface potential. Since no structural changes were detected in the ground state of the mutant D96G (Subramaniam et al., 1993), this cause does not seem to be very likely. A charge on Asp-96 would need to be stabilized by a counterion and/or delocalized by hydrogen bonds. The possibility for an ion pair with Arg-227 was suggested on the basis of the observed slow M-decay found for the mutant R227Q (Stern & Khorana, 1989). The substitution of Asp-96 with Asn is affecting not only the later but also the early part of the photocycle, suggesting a structural role for Asp-96 (Thorgeirsson et al., 1991). Results from FTIR spectroscopy clearly show perturbations during the formation of the L and M intermediates interpreted as conformational changes (Gerwert et al., 1989) or protonation changes (Braiman et al., 1988). Furthermore,

strong hydrogen bond changes are detected during the K to L transition (Maeda et al., 1992). If Asp-96 does play a structural role, an ion pair would be the most likely arrangement. For the presumed functional role of Asp-96 as proton donor for the Schiff base in the M to N transition, Asp-96 must become protonated at or before the M-state.

It is of interest to compare our results for the charge of each side of bR with those expected, based on the model for the secondary structure of Figure 1. Such a calculation of the net surface charge contains an element of arbitrariness. Which groups should be included? Should full charges or only partial charges be used at pH 6.6? How should the contribution of charges buried in the protein be weighted? Clearly, the results of this simplified calculation should be regarded with caution. Taking into account our results for Lys-129, we obtained a net negative charge of two elementary charges for the extracellular side, assuming contributions from Glu-9,74,-194,204; Asp-85; Arg-7,82,134; and Asp-212 as the counterion to the protonated Schiff base. Considering our results for Asp-96 and the C-terminal tail, we found a net charge of one negative charge for the cytoplasmic side, assuming contributions from Asp-36,38,96,102,104; Glu-161,166; Arg-164,-227,225; Lys-30,40,41,159,172; and the C-terminal tail (2 e^-). The calculation shows that the expected net surface charge is small due to extensive cancellation. The values determined with the bound fluorescein of approximately 1.8 negative charges for the extracellular side and 2.5 negative charges for the cytoplasmic side are thus within the expected range.

REFERENCES

Altenbach, C., Marti, T., Khorana, H. G., & Hubbell, W. L. (1990) *Science 248*, 1088–1092.

Braiman, M. S., Mogi, T., Marti, T., Stern, L. J., Khorana, H. G., & Rothschild, K. J. (1988) *Biochemistry 27*, 8516–8520.

Cevc, G. (1990) *Biochim. Biophys. Acta 1031*, 311–382.

de Groot, H. J. M., Smith, S. O., Courtin, J., van den Berg, E., Winkler, C., Lugtenburg, J., Griffin, R. G., & Herzfeld, J. (1990) *Biochemistry 29*, 6873–6883.

Dér, A., Száraz, S., Tóth-Boconádi, R., Tokaji, Zs., Keszthelyi, L., & Stoeckenius, W. (1991) *Proc. Natl. Acad. Sci. U.S.A. 88*, 4751–4755.

Ebrey, T. G. (1993) in *Thermodynamics of Membrane Receptors and Channels* (Jackson, M. B., Ed.) pp 353–387, CRC Press, Boca Raton, FL.

Ehrenberg, B., Ebrey, T. G., Friedman, N., & Sheves, M. (1989) *FEBS Lett. 250*, 179–182.

Flitsch, S. L., & Khorana, H. G. (1989) *Biochemistry 28*, 7800–7805.

Gerwert, K., Hess, B., Soppa, J., & Oesterhelt, D. (1989) *Proc. Natl. Acad. Sci. U.S.A. 86*, 4943–4947.

Henderson, R., Baldwin, J. M., Ceska, T. A., Zemlin, F., Beckmann, E., & Downing, K. H. (1990) *J. Mol. Biol. 213*, 899–929.

Honig, B., & Hubbell, W. L. (1984) *Proc. Natl. Acad. Sci. U.S.A. 81*, 5412–5416.

Jonas, R., Koutalos, Y., & Ebrey, T. G. (1990) *Photochem. Photobiol. 52*, 1163–1177.

Kates, M., Kushawa, S. C., & Sprott, G. D. (1982) *Methods Enzymol. 88*, 98–111.

Kimura, Y., Fujiwara, & Ikegami, A. (1984) *Biophys. J. 45*, 615–625.

Koutalos, Y., Ebrey, T. G., Gilson, H. R., & Honig, B. (1990) *Biophys. J. 58*, 493–501.

London, E., & Khorana, H. G. (1982) *J. Biol. Chem. 257*, 7003–7011.

Maeda, A., Sasaki, J., Shichida, Y., & Yoshizawa, T. (1992) *Biochemistry 31*, 462–467.

Marti, T., Rösselet, S. J., Otto, H., Heyn, M. P., & Khorana, H. G. (1991) *J. Biol. Chem. 266*, 18674–18683.

Mathies, R. A., Lin, S. W., Ames, J. B., & Pollard, W. T. (1991) *Annu. Rev. Biophys. Chem. 20*, 491–518.

Metz, G., Siebert, F., & Engelhard, M. (1992) *Biochemistry 31*, 455–462.

Miller, A., & Oesterhelt, D. (1990) *Biochim. Biophys. Acta 1020*, 57–64.

Mogi, T., Stern, L. J., Marti, T., Chao, B. H., & Khorana, H. G. (1988) *Proc. Natl. Acad. Sci. U.S.A. 85*, 4148–4152.

Ormos, P., Chu, K., & Mourant, J. (1992) *Biochemistry 31*, 6933–6937.

Otto, H., Marti, T., Holz, M., Mogi, T., Lindau, M., Khorana, H. G., & Heyn, M. P. (1989) *Proc. Natl. Acad. Sci. U.S.A. 86*, 9228–9232.

Otto, H., Marti, T., Holz, M., Mogi, T., Stern, L. J., Engel, F., Khorana, H. G., & Heyn, M. P. (1990) *Proc. Natl. Acad. Sci. U.S.A. 87*, 1018–1022.

Ovchinnikov, Yu. A., Abdulaev, N. G., Feigina, M. Yu., Kiselev, A. V., & Lobanov, N. A. (1977) *FEBS Lett. 84*, 1–4.

Packer, L., Arrio, B., Johannin, G., & Volfin, P. (1984) *Biochem. Biophys. Res. Commun. 122*, 252–258.

Papadopoulos, G., Dencher, N. A., Zaccai, G., & Büldt, G. (1990) *J. Mol. Biol. 214*, 15–19.

Renthal, R., & Cha, C.-H. (1984) *Biophys. J. 45*, 1001–1006.

Stern, L. J., & Khorana, H. G. (1989) *J. Biol. Chem. 24*, 14202–14208.

Subramaniam, S., Marti, T., & Khorana, H. G. (1990) *Proc. Natl. Acad. Sci. U.S.A. 87*, 1013–1017.

Subramaniam, S., Gerstein, M., Oesterhelt, D., & Henderson, R. (1993) *EMBO J. 12*, 1–8.

Szundi, I., & Stoeckenius, W. (1988) *Biophys. J. 54*, 227–232.

Szundi, I., & Stoeckenius, W. (1989) *Biophys. J. 56*, 369–383.

Taneva, S., Todorov, G., Petkanchin, I. B., & Stoylov, S. P. (1987) *Eur. Biophys. J. 14*, 415–421.

Thorgeirsson, T. E., Milder, S. J., Miercke, L. J. W., Betlach, M. C., Shand, R. F., Stroud, R. M., & Kliger, D. S. (1991) *Biochemistry 30*, 9133–9142.

Tittor, J., Soell, Ch., Oesterhelt, D., Butt, H.-J., & Bamberg, E. (1989) *EMBO J. 8*, 3477–3482.

Tsujimoto, K., Yorimitsu, S., Takahashi, T., & Ohashi, M. (1989) *J. Chem. Soc., Chem. Commun.*, 668–670.

Warshel, A., Russell, S. T., & Churg, A. K. (1984) *Proc. Natl. Acad. Sci. U.S.A. 81*, 4785–4789.